energies

MDPI

Article

In Situ Stress Determination Based on Acoustic Image Logs and Borehole Measurements in the In-Adaoui and Bourarhat Hydrocarbon Fields, Eastern Algeria

Rafik Baouche [1], Souvik Sen [2,†], Ahmed E. Radwan [3,*] and Ahmed Abd El Aal [4]

[1] Laboratory of Resources Minérals at Energétiques, Department of Geophysic, Faculty of Hydrocarbons and Chemistry (FHC), University M'Hamed Bougara Boumerdes, Boumerdes 35000, Algeria
[2] Geologix Limited, Dynasty Building, Andheri Kurla Road, Andheri (E), Mumbai 400059, Maharashtra, India
[3] Faculty of Geography and Geology, Institute of Geological Sciences, Jagiellonian University, Gronostajowa 3a, 30-387 Kraków, Poland
[4] Civil Engineering Department, College of Engineering, Najran University, Najran 1988, Saudi Arabia
* Correspondence: radwanae@yahoo.com or ahmed.radwan@uj.edu.pl
† Current address: Reservoir Technical Services, Baker Hughes, Mumbai 400703, Maharashtra, India.

Abstract: The study of in situ stress from image logs is a key factor for understanding regional stresses and the exploitation of hydrocarbon resources. This work presents a comprehensive geomechanical analysis of two eastern Algerian hydrocarbon fields to infer the magnitudes of principal stress components and stress field orientation. Acoustic image logs and borehole measurements were used in this research to aid our understanding of regional stress and field development. The studied In-Adaoui and Bourarhat fields encompass a combined thickness of 3050 m of Paleozoic and Mesozoic stratigraphy, with the primary reservoir facies in the Ordovician interval. The Ordovician sandstone reservoir interval indicates an average Poisson's ratio (v) of 0.3, 100–150 MPa UCS, and 27–52 GPa Young's modulus (E). Direct formation pressure measurements indicate that the sandstone reservoir is in a hydrostatic pore pressure regime. Density-derived vertical stress had a 1.1 PSI/feet gradient. Minimum horizontal stress modeled from both Poisson's ratio and an effective stress ratio-based approach yielded an average 0.82 PSI/feet gradient, as validated with the leak-off test data. Drilling-induced tensile fractures (DITF) and compressive failures, i.e., breakouts (BO), were identified from acoustic image logs. On the basis of the DITF criterion, the maximum horizontal stress gradient was found to be 1.57–1.71 PSI/feet, while the BO width-derived gradient was 1.27–1.37 PSI/feet. Relative stress magnitudes indicate a strike-slip stress regime. A mean S_{HMax} orientation of N130°E (NW-SE) was interpreted from the wellbore failures, classified as B-quality stress indicators following the World Stress Map (WSM) ranking scheme. The inferred stress magnitude and orientation were in agreement with the regional trend of the western Mediterranean region and provide a basis for field development and hydraulic fracturing in the low-permeable reservoir. On the basis of the geomechanical assessments, drilling and reservoir development strategies are discussed, and optimization opportunities are identified.

Keywords: geomechanical characterization; in situ stress; Lower Turonian; unconventional reservoir; tight carbonates; fracture reactivation; Constantine Basin

Citation: Baouche, R.; Sen, S.; Radwan, A.E.; Abd El Aal, A. In Situ Stress Determination Based on Acoustic Image Logs and Borehole Measurements in the In-Adaoui and Bourarhat Hydrocarbon Fields, Eastern Algeria. *Energies* **2023**, *16*, 4079. https://doi.org/10.3390/en16104079

Academic Editor: Ernst Huenges

Received: 9 February 2023
Revised: 3 April 2023
Accepted: 6 May 2023
Published: 13 May 2023

1. Introduction

Principal stresses and formation pressure have a direct impact on drilling, wellbore stability, and production optimization [1–5]. Accurate interpretation of stress field orientation contributes to optimal deviated and horizontal well placement, hydraulic fracturing design, and an improved understanding of complex faulting systems and local stress field perturbations [6–8]. A comprehensive geomechanical model integrating wireline logs, drilling data, and subsurface measurements has become a primary requirement to address

the well-related challenges and minimize non-productive times and cost overruns from exploration to abandonment [9,10].

A geomechanical model contributes to the confident assessment of rock strength, elastic properties, formation pore pressure distribution, in situ stress magnitudes, and horizontal stress orientations. Horizontal stress azimuths are inferred from compressive and tensile wellbore failure features from image logs, four-arm caliper logs, earthquake focal mechanism, etc. Conventionally wireline logs and necessary geological datasets are utilized to estimate various geomechanical model parameters, which are then calibrated and validated with direct downhole measurements, core-based rock-mechanical measurements, and various drilling-event-based inferences. Among the three in situ stresses, the vertical stress (Sv) and minimum horizontal stress (S_{hmin}) are easier to estimate and usually validated with various commonly available downhole measurements (e.g., leak-off test, extended leak-off test, mud loss events during drilling). Maximum horizontal stress (S_{HMax}) is the most difficult to quantify [11]. However, image logs are one of the best ways to confidently infer and constrain S_{HMax} magnitudes from borehole failures. Previous researchers worked on the geomechanical aspects of various Algerian hydrocarbon provinces, i.e., Illizi Basin [3,4,9,12,13], Oued Mya Basin [14], Constantine Basin [15,16], Berkine Basin [17], and the Hassi Messaoud fields [18]. The geomechanical characteristics and in situ stress magnitudes and orientations in the In-Adaoui and Bourarhat hydrocarbon fields are vital for field development and future hydraulic fracturing, but no prior studies have been conducted in this area, which sets the premise of this study.

In this regard, we conducted a well-based geomechanical assessment of two hydrocarbon fields in the eastern Algeria. We studied the onshore exploratory and appraisal wells drilled in the In-Adaoui and Bourarhat hydrocarbon fields. The studied wells cover a maximum of 3050 m of Paleozoic and Mesozoic stratigraphy and primarily target the Ordovician sandstone reservoirs. The key objective of this work was to quantitatively assess the principal stresses and compare the in-situ stress results to the present-day tectonic stress field and stress field orientation. Wireline data consisting of gamma ray, density, resistivity, compressional, and shear sonic slowness logs were the primary input parameters behind this geomechanical analysis. Direct formation pressure measurements (MDT), drilling data (mud weight, leak-off test), and an acoustic image log recorded by the ultrasonic borehole imaging tool (UBI) were available and utilized to infer and calibrate various subsurface pressure magnitudes. The availability of breakouts and drilling-induced tensile fractures provided a critical and confident interpretation of S_{HMax}, which is scarce in the eastern Algerian basins.

2. Geological Setting

The studied In-Adaoui and Bourarhat fields are situated in the Illizi Basin, eastern Algeria (Figure 1). This intra-cratonic basin was formed in the Paleozoic. The basin is located close to the border between Libya and Algeria. Its western boundary is defined by the Amguid-Hassi Touareg structural axis [19], while the eastern boundary is defined by the Tihemboka Arch [2]. Hoggar Massif is located on the southern side of the Illizi Basin [19]. This region of the Saharan platform exhibits near flat structural dip and is regarded to be majorly affected by strike-slip tectonics [2]. We analyzed data from two oil fields, namely, In-Adaoui and Bourarhat. In-Adaoui field is situated to the north of Bourarhat field. The Paleozoic stratigraphy of the study area is characterized by sandstone, siltstone, and shale intercalations that were deposited during several transgressive and regressive cycles [2]. The Paleozoic reservoirs of the Illizi Basin are dominantly quartz arenites of glacial, tidal shallow marine origin that were deposited as the Ordovician lowstand system tract. Silurian transgressive marine shale is considered the source rock contributing to the hydrocarbon accumulation in the Ordovician glaciogenic sandstones [19]. These marine Silurian shales contain 2–4% organic content. The Devonian unit lies unconformably above the Silurian unit and is composed of deltaic, fluvial, and shallow marine sandstone reservoirs, as reported from various parts of the Illizi Basin and nearby Paleozoic oil fields.

Upper Carboniferous marks the regional Hercynian unconformity in the studied fields over which Mesozoic sediments were deposited. A lithostratigraphic chart of the fields was prepared from the drill cutting description, well log correlation, and regional geological information [19], as presented in Table 1. In the In-Adaoui field, the top of the Ordovician formation is established at approximately 2890 m TVD (true vertical depth), while in the Bourarhat field, it is encountered at a much shallower depth, around 2160 m TVD, due to the uplift and erosion of the entire Mesozoic sequence in the Bourarhat region during the Upper Carboniferous Hercynian orogenesis. Both fields are associated with NW-SE trending regional faults.

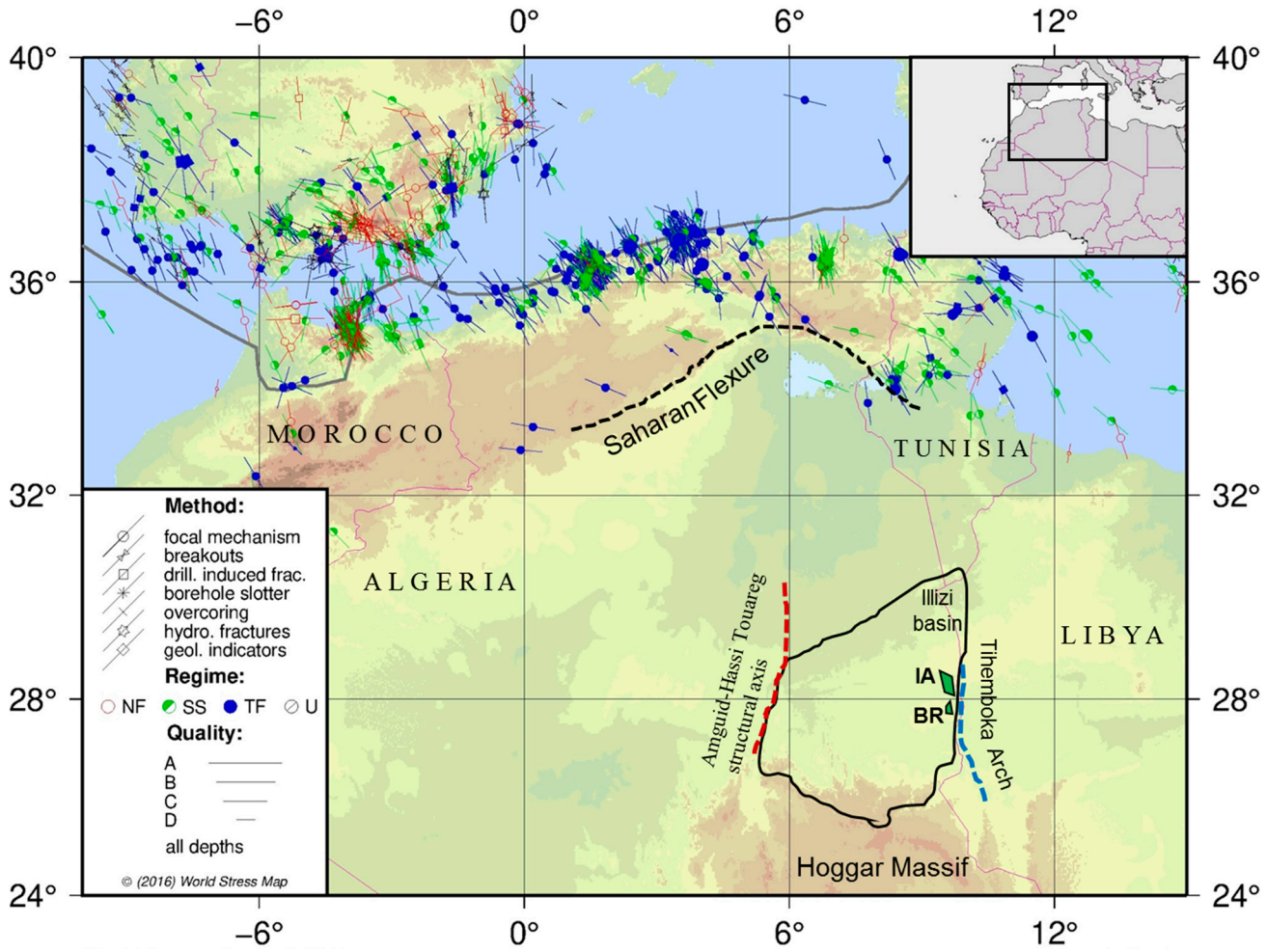

Figure 1. Location map of the two studied fields, namely, In-Adaoui (IA) and Bourarhat (BR), as marked by green color. The map is prepared by using CASMI, a tool for the WSM database accessed by the online interface CASMO [20].

Table 1. Lithostratigraphic chart of the In-Adaoui and Bourarhat fields, as encountered in the studied wells.

System	Stage/Formation	Dominant Lithology
Cretaceous	Senonian Cenomanian	Gypsum, mixed carbonate-clastic
	Albian Aptian Barremian	Sandstone, minor shale
Jurassic	Malm Dogger Lias	Sandstone–shale intercalations
Triassic	Keuper	Sandstone, minor shale, dolomite
unconformity		
Carboniferous	Westphalian	Carbonate, shale
	Mamurian	Clastics, minor carbonate
Lower Carboniferous	Visean B–C Tournasian	Shale, minor sandstone
Devonian	Strunian	Sandstone–shale intercalations
	Fammenian Frasnian	Shale dominated
	Devonian	Sandstone dominated
Silurian	Silurian	Sandstone dominated
	Silurian Argileux	Shale dominated
Ordovician	Unit IV–III	Sandstone/quartzite reservoir, minor shale

3. Materials and Methods

This study integrated wireline logs, drilling data, and downhole measurements from two vertical wells (Well-1 from Bourarhat field and Well-2 from In-Adaoui field) to interpret the mentioned deliverables. Horizontal stress orientations were interpreted from the wellbore failures. If the stresses around the wellbore exceed the rock's strength, rock will fail. Stress concentration is most compressive in the direction of minimum horizontal stress. If the differential pressure on the wellbore wall (i.e., difference between pore pressure and drilling fluid pressure) increases and hoop stress decreases, the wellbore wall can locally go into tension along the maximum horizontal stress orientation, resulting in a tensile crack. When circumferential hoop stress in a vertical borehole exceeds the rock's compressive strength, breakouts occur parallel to the S_{hmin} direction. Alternatively, a circumferential hoop stress that exceeds (is more negative than) the rock's tensile strength results in DITF parallel to the S_{HMax} azimuth. The most reliable way to observe wellbore breakouts (BO) is through the use of acoustic image logs, which exhibit breakouts as dark bands of low reflectance on opposite sides of the wellbore wall [1]. DITF does not propagate large distance away from the wellbore wall (few centimeters) and therefore it does not contribute to any drilling risk (mud loss, etc.). Therefore, image logs are the only way to detect if any tensile failures were created on wellbore wall induced by drilling.

The quality of these failure features is classified as per the World Stress Map (i.e., WSM) ranking guidelines [20], and mean stress orientations are interpreted for the study area. An estimate of the vertical stress (S_v) is generated from the wireline bulk-density log [21] using the following expression:

$$S_v = \int_0^z \rho(z) g \, dz \quad (1)$$

where $\rho(z)$ denotes the rock density at depth (z) available from wireline bulk-density log, and 'g' is the gravitational acceleration (9.8 m/s^2). Due to the unavailability of a density log

at the surface hole section, a regional density trend (power law curve) was utilized to fill the data gap. The density trend was appended with the wireline data to generate a composite density curve for the entire well [11,22,23]. Pore pressure (PP) against the Ordovician sandstone reservoir interval was interpreted from the direct downhole measurements. Due to the intercalating sandstone–siltstone–shale lithostratigraphy, drilling mud weight was used as a pore pressure proxy in the studied wells. Usually, downhole mud weight is kept above the formation pore pressure to avoid any fluid influx from the formation into the wellbore [24–28]. On the basis of the S_v and PP, S_{hmin} and S_{HMax} were modeled. We employed the Mathews and Kelly method [29] to estimate S_{hmin} magnitude:

$$S_{hmin} = K * (S_v - PP) + PP \tag{2}$$

where K is the effective stress ratio, deduced from the leak off test (LOT). We also applied the Poisson's ratio-based Eaton's method [30]:

$$S_{hmin} = PP + \frac{\upsilon}{1-\upsilon}(S_v - PP) \tag{3}$$

where υ is the Poisson's ratio (unitless), estimated from compressional and shear wave velocities. Wellbore breakouts were identified from the acoustic image log recorded by the ultrasonic borehole imaging tool (UBI). Interactive display processing allows cross-sections of a wellbore to be easily displayed in an unwrapped imager view, thus making it straightforward and easy to demarcate the opening angle of breakout, also known as breakout width. BO occurs systematically on both sides of the wellbore wall. However, during image log analysis, the widths and orientations of the BOs were picked and documented separately. For a particular BO feature, an average of width and orientation can be considered representative. S_{HMax} magnitude is estimated from breakout widths [31]:

$$S_{HMax} = \frac{\left[\left(UCS + 2PP + \Delta p + \sigma^{\Delta T}\right) - \left(S_{hmin}(1 + 2\,Cos\,(\pi - BO_{Width})\right)\right]}{1 - 2\,Cos\,(\pi - BO_{Wdith})} \tag{4}$$

where Δp indicates the differential pressure (mud pressure-pore pressure), UCS denotes the unconfined compressive strength (PSI), $\sigma^{\Delta T}$ is the thermal stress (PSI), and BO_{Width} is the width of the breakout (in radians), as interpreted from the image logs.

The entire stratigraphy encountered in the studied wells was sandstone and shale, and therefore we utilized the following equations to estimate UCS [32,33] from compressional sonic slowness log (DTC):

$$Sandstone: UCS = 1200 * 145.038 * \ e^{-0.036 * \ DTC} \tag{5}$$

$$Shale: UCS = 0.77 * 145.038 * \left(\frac{304.8}{DTC}\right)^{2.93} \tag{6}$$

where UCS and DTC are in PSI and μs/ft units, respectively. Zoback et al. [34] and Zoback [1] 07) proposed another method to estimate S_{HMax} if drilling induced tensile fractures (DITF) are present:

$$S_{HMax} = 3S_{hmin} - 2PP - \Delta p - T_o - \sigma^{\Delta T} \tag{7}$$

where T_o is the tensile strength of the rock. In our studied wells, both breakouts and DITF were identified, and therefore we used both the approaches (Equations (3) and (7)) to estimate S_{HMax}. However, we considered thermal stress to be negligible. Moreover, due to the unavailability of the multiple cycles of the extended LOT, we assumed the rock tensile strength to be 10% of the compressive strength.

4. Results and Discussion

4.1. Acoustic Image Log Analysis

Compressive and tensile wellbore failures were identified from the visual inspection of the acoustic image logs recorded in the Ordovician reservoir section in the Bourarhat field, as presented in Figure 2. Breakouts (BO), the compressive failures, appeared as two broad, parallel failure zones, 180° apart and characterized by low acoustic amplitudes along the NE-SW azimuth (refer to the wide, low amplitude black patches on the unwrapped UBI panels in Figure 2). Drilling induced tensile fractures (DITF) appeared as a parallel set of two narrow failure lines (i.e., hairline) along NW-SE, at 90° apart from the BO zones. A minimum failure length of 1 m was considered for the assessment. Thirteen distinct BO zones with cumulative length of approximately 90 m were observed in a single well, while a combined 150 m of DITF was observed as eight different zones. Both failures yielded a standard deviation of $\leq$20°, and therefore both failures were classified as B-quality stress indicators following the WSM ranking scheme. A mean S_{HMax} orientation of N130°E was interpreted in the study area, which was parallel to the movement direction of the Eurasian and African plates. The inferred horizontal stress orientations were in good agreement with the published data from the Tinzaouatine field [2,13], Oued Mya field [14], and Hassi Messaoud fields [18].

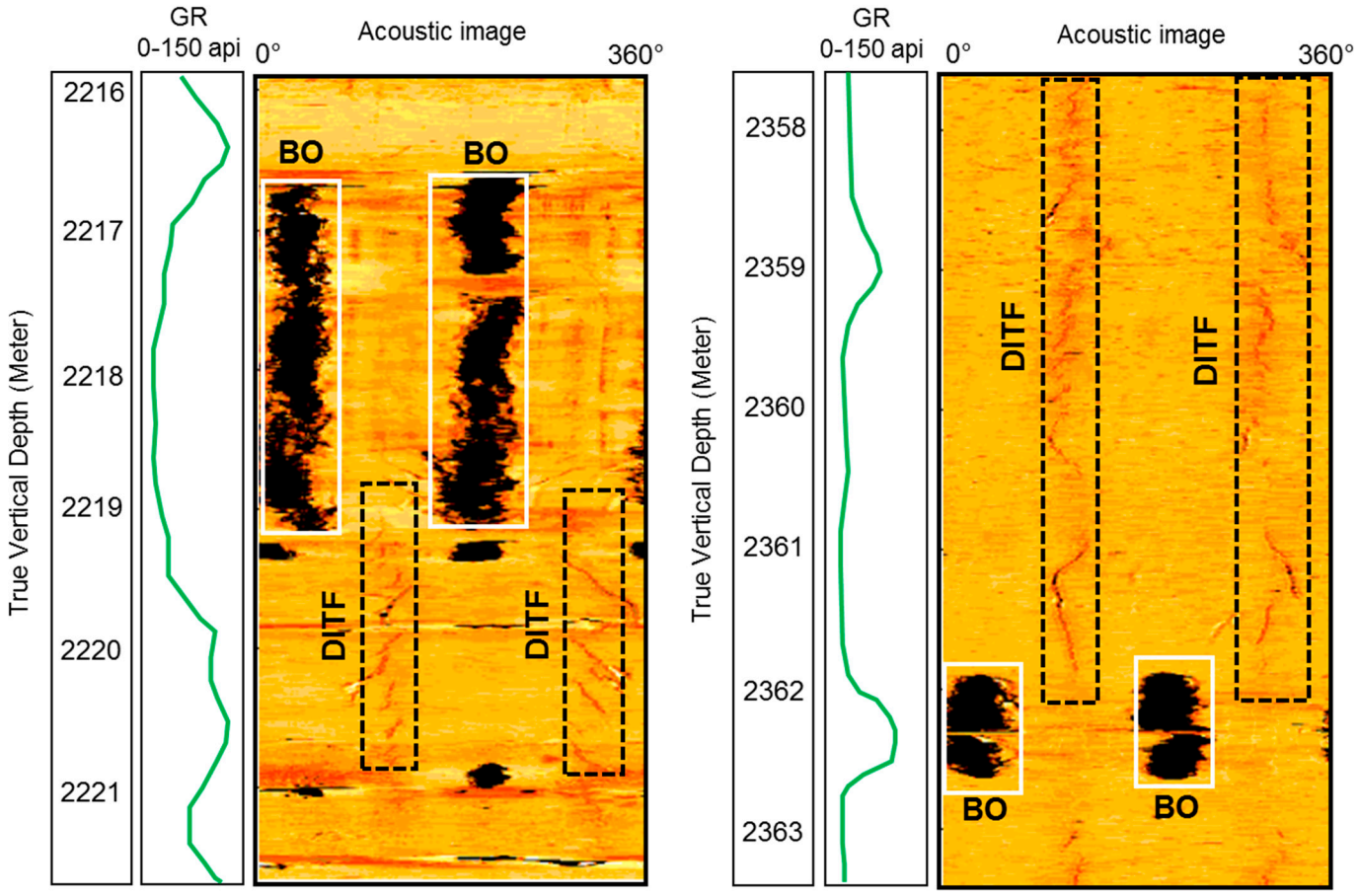

Figure 2. The acoustic image log (UBI) recorded in the Ordovician sandstone reservoir interval, Well-1, Bourarhat field (vertical well, maximum recorded inclination 2°). Both the compressive (BO) and tensile (DITF) failures were observed and utilized to interpret horizontal stress orientation as well as S_{HMax} magnitude. DITFs were seen along NW-SE, and BOs occurred along the NE-SW azimuth. GR denotes gamma ray log (unit: api).

4.2. Rock Mechanical Model

Rock mechanical properties were estimated from the bulk-density, compressional, and shear slowness logs available from the wireline log suite. It is noticed that the depth interval from 2200 to 2320 m had a slight difference in log response from the depth interval of 2320 to 2450 m. The depth interval of 2320 to 2450 m had more consistent values in slowness response, while the depth interval of 2200 to 2320 m had an irregular response in slowness, density, and elastic parameters. The slowness showed a varied response within the Ordovician sandstone reservoir, and the highest slowness was detected in the top part of the formation. Consequently, the UCS and elastic parameters depended on compressional slowness and showed the same response. The Ordovician sandstone reservoir interval indicated an average Poisson's ratio (v) of 0.3, 100–150 MPa UCS, and 27–52 GPa Young's modulus (E) (Figure 3). The depth interval of 2320 to 2450 m had more consistent values in the base, but it was denser in the top part. Due to the unavailability of the core-based laboratory measurements, the calculated rock mechanical properties may have had some uncertainties; however, the inferred values were well correlated with the regional data published by English et al. [9], where the authors reported a 41–58 GPa Young's modulus and 90–170 MPa UCS based on the core-based uniaxial test measurements of Ordovician sandstones.

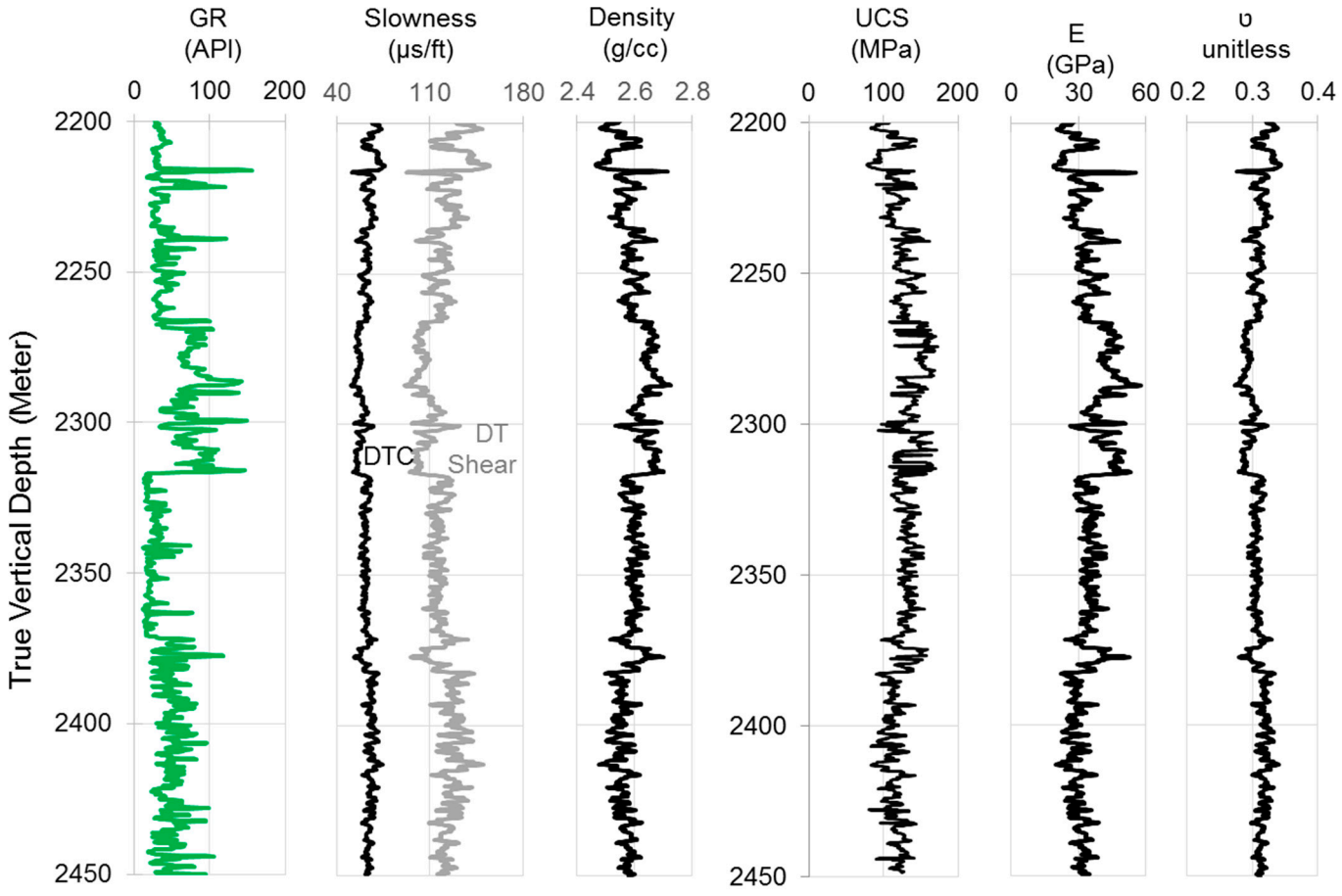

Figure 3. The wireline log-derived elastic properties and compressive strength against the Ordovician sandstone reservoir interval, Bourarhat field.

4.3. Borehole Measurments

Interpreted pressure magnitudes are presented in Figure 4. Sv derived from the bulk-density log had a gradient of about 1.1 PSI/feet. We compared the Sv gradient with the reported S values from other fields in Algeria. Baouche et al. [2] reported an average Sv gradient of 2.07 PI/feet from the eastern Illizi Basin, while a 1.02 PSI/feet Sv gradient

was reported from the Hassi Messaoud field by Baouche et al. [18]. A marginally higher Sv gradient of 1.12 PSI/ft (≈25.33 MPa/km) was reported from the Tinzaouatine field, Illizi Basin [13]. Similar Sv gradients were also reported from the Hassi Berkine South field [18] and the Tinzaouatine field, Illizi Basin [13]. The direct downhole formation pressure measurements (MDT) inferred a 0.44 PSI/feet gradient in the Ordovician reservoir interval, which corroborated well with the observations by Baouche et al. [2] from other fields in the Illizi Basin.

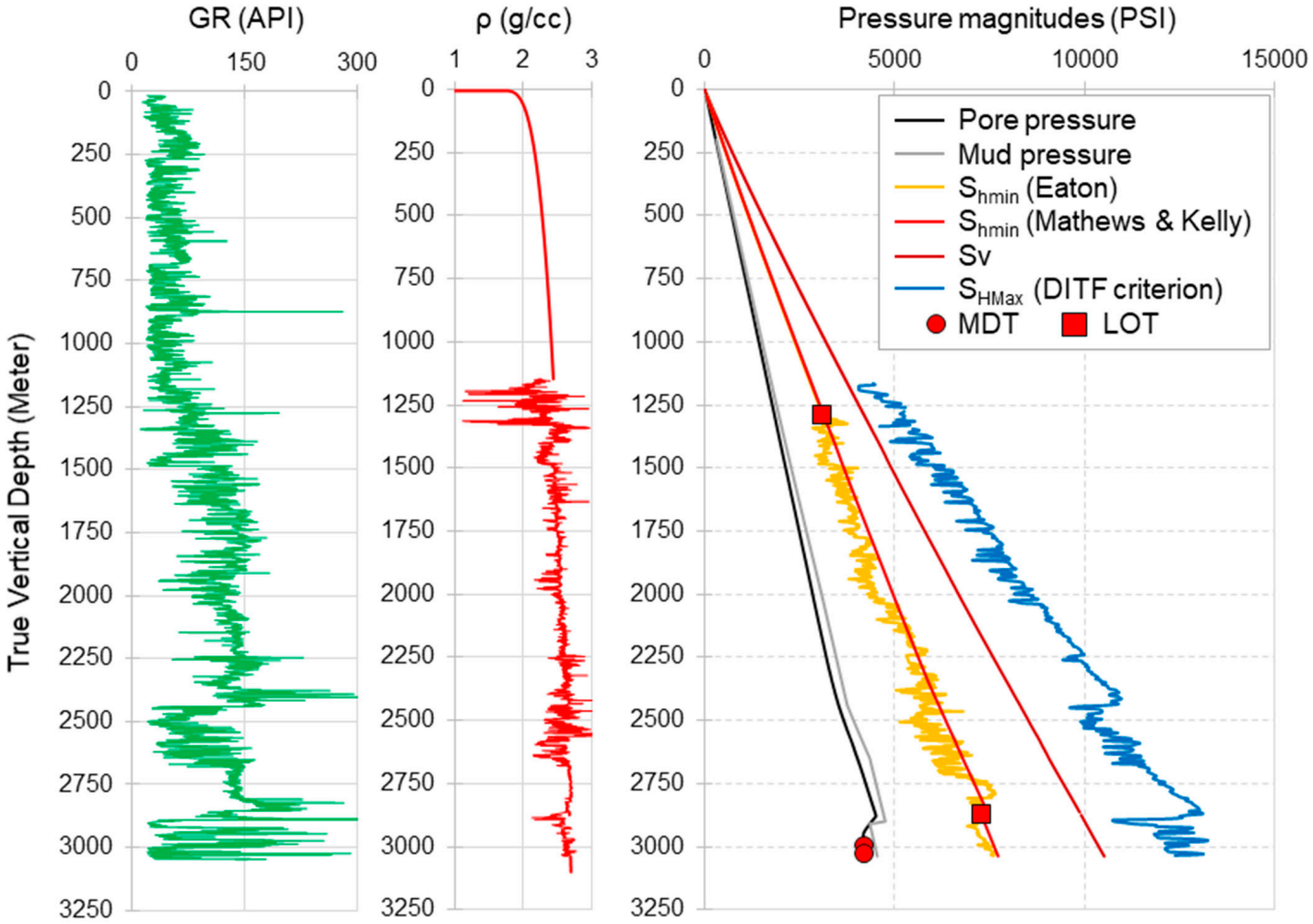

Figure 4. The gamma ray and density logs along with the pore pressure and principal stress profiles of the Well-2, In-Adaoui field. Pore pressure against the Ordovician reservoir is interpreted from direct measurements by the MDT tool. Shmin was estimated by two methods (Eaton's and Mathews and Kelly), validated with LOT points. S_{HMax} was estimated from the DITF-based estimation method.

The Devonian–Cretaceous clastic succession had a hydrostatic pressure gradient. The Silurian shale was interpreted to have 0.66 PSI/feet gradient. This interpretation is based on the drilling mud weight proxy, considering drilling maintained sufficient downhole overbalance, as no connection gas or formation fluid influx events were reported. Similar pore pressure gradients in the Silurian and Ordovician pore pressure gradients were observed in the literature [2,12] from the nearby Takouazet field. From the LOTs, an effective stress ratio of 0.55 (K value in Equation (2)) was deciphered and used in the S_{hmin} estimation by the Mathews and Kelly method. On the basis of both the methods (Equations (2) and (3)), a mean S_{hmin} gradient of 0.82 PSI/feet was interpreted in the Paleozoic and Mesozoic stratigraphy of the In-Adaoui and Bourarhat fields. English et al. [9] studied the fracture closure pressure data of Ordovician intervals from Illizi Basin and provided a wide S_{hmin} gradient range of 0.62–0.86 PSI/feet, and our results were in good agreement with this

observation. Baouche et al. [13] inferred a S_{hmin} gradient range of 0.77–0.83 PSI/feet in the Tinzaouatine field (located in the south of our studied fields) on the basis of the C-quality minifrac measurements and the coexistence of BO and DITF in image logs. It is to be noted that fracture closure pressure provided the best estimate for S_{hmin}. Since LOT values are generally higher than closure pressure, our LOT-calibrated S_{hmin} can be considered as an upper limit for minimum horizontal stress.

4.4. Stress Regime

In this study, S_{HMax} magnitude was estimated from both the compressive as well as tensile failures, as presented in Figure 5. S_{hmin} estimated from the Mathews and Kelly method was utilized in Equations (4) and (6) for quantifying S_{HMax}. On the basis of the presence of DITF and with the assumption of negligible thermal stress, the S_{HMax} gradient was found to be 1.57–1.71 PSI/feet. It is to be noted that the accurate values of rock tensile strength were unavailable due to the lack of extended LOT data. Average BO widths of 45–50° were dominantly found in the acoustic image log, which provided a 1.27–1.37 PSI/feet S_{HMax} gradient in the Ordovician interval. We compared our S_{HMax} results with those of Baouche et al. [13], where the authors analyzed the coexistence of BO and DITF in the acoustic image log and inferred a S_{HMax} gradient ranging between 1.25 and 1.7 PSI/feet in the Tinzaouatine field, eastern Illizi Basin.

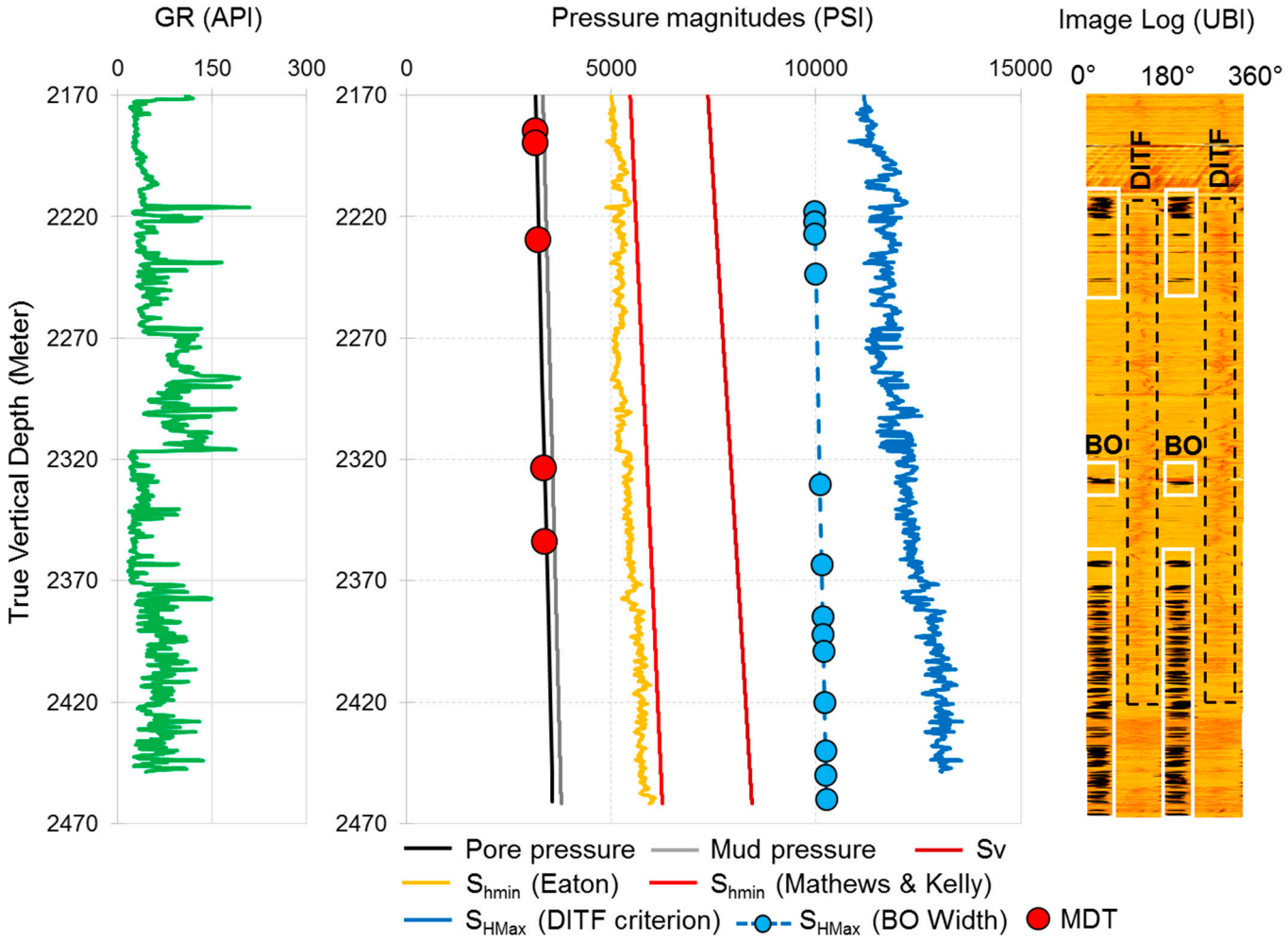

Figure 5. The reservoir pore pressure and principal stress profiles in the Bourarhat field. S_{HMax} was estimated by two methods employing both the compressive (breakout, i.e., BO) and tensile (DITF) failures. BO and DITF trends are marked on the acoustic image log (UBI tool) on the right most panel by solid blue and dotted white rectangle, respectively.

Uncertainty in this result may be contributed by the lack of direct UCS measurements. However, we already discussed that our calculated UCS was in close range with English et al. [9], which yielded a higher degree of confidence in our model. The second source of uncertainty was due to thermal stress. This was a difficult parameter to model, and therefore assumed it to be negligible [1]. The inferred S_{HMax} gradient range matched well with the results from English et al. [9], where the authors reported a maximum S_{HMax} gradient of 1.4 PSI/feet from the Ordovician interval of the Illizi Basin, located to the south of our studied fields. It was observed that the S_{HMax} magnitudes estimated from the DITF were higher than the same results from BO width. The results suggest that the stress state in the studied fields was strike-slip ($S_{HMax} > S_v > S_{hmin}$). Moreover, the occurrence of DITF in the vertical well was a characteristic of the strike-slip tectonic regime [1,35].

4.5. Implications for Regional Stress and Field Development

In the North Africa region, a major strike-slip fault system was active, starting in the Cretaceous [36–38]. Heidbach et al. [36] show a first-order stress pattern in the North Africa region based on the World Stress Map database, and they inferred that the first-order S_{HMax} orientation is fairly consistent with the relative plate motion of Africa with respect to Eurasia. They indicate that the large tectonic forces played the key role in the first-order stress pattern, but numerous small S_{Hmax} perturbations may occur due to other stress sources (i.e., mostly third order) [37–39]. Soumaya et al. [39] studied the complex strike-slip system along the northern Africa region (i.e., the Western Mediterranean), starting from Tunisia to Morocco, and they studied the active faulting geometry and their stress pattern. The smoothed stress map highlighted the mean S_{HMax} orientation (N148° E ± 10.4°) in the North Africa region (i.e., the Western Mediterranean); in addition, the geodetic model [40] refers to the mean S_{HMax} orientation (N134° E ± 15°). In our study, a mean S_{HMax} orientation of N130°E was interpreted in the study area, which was parallel to the movement direction of the Eurasia and African plates. Although the location of the In-Adaoui and Bourarhat hydrocarbon fields was far to the south, it contributed to our understanding about the in situ stresses in the region. Breakouts were commonly observed in the studied wells. Mitigating breakouts usually require a higher mud weight above the formation collapse pressure. It is to be noted that a high horizontal stress contrast (as in our case) in a strike slip domain usually means failures are likely to occur. Vertical wells are the most unstable ones in a strike-slip regime, while horizontal wells are more stable in comparison. In terms of horizontal well drilling, a drilling direction parallel to minimum horizontal stress requires more mud weight and is therefore more challenging when drilling towards the S_{HMax} azimuth. Our in-situ stress research indicates that the In-Adaoui and Bourarhat hydrocarbon fields' future field development wells need to be drilled parallel to the Shmin azimuth (i.e., NE-SW). The hydraulic fracture operation can be managed to help by drilling the development wells in a NE-SW direction. This will allow the hydraulic fractures to spread along the S_{HMax} direction and effectively create a transverse fracture network within the Ordovician reservoirs, which typically have low permeability. Drilling long laterals usually yields hole-cleaning issues. The best hole-cleaning procedures need to be maintained to avoid cutting accumulation on the lower side of the lateral. A close monitoring of torque and drag behavior and downhole equivalent circulation density (ECD) during drilling (using real time logging while drilling data) is critical in such cases. Annular loading by cutting build-up induced by insufficient hole cleaning has critical implications for the wellbore's stability. Accordingly, high viscosity sweeps, wiper trips, and circulation bottoms up can be applied to lift the cuttings after regular drilling intervals.

Since the studied Paleozoic sandstones are not highly porous and permeable, we do not envisage any potential risk of differential sticking due to the high mud weight, which is required to tackle wellbore compressive failures. Moreover, the overall high rock strength (>100 MPa) may indicate a lesser chance of solid production during initial production-induced depletion. However, a detailed modeling of critical bottomhole flowing pressure is to be performed in order to assess the sanding risks during the later stages of

production. On the basis of the acoustic slowness and estimated rock strength signatures within the targeted Ordovician sandstone interval, we inferred variations in compressive strength; for example, the highest slowness was detected in the top part of the formation. Such variations can result from grain packing, cementation effects, or the presence of clay mineralogy within the stacked sandstone bodies. Considering the requirement of horizontal wells to develop these tight reservoirs, if such rock strength variations are encountered along the lateral section, it will result in ledges at the bed boundaries (high vs. low rock strength). Tight hole challenges can be expected in such cases during tripping. Excessive hard back-reaming is to be avoided to tackle such tight holes. We conclude that drilling optimization in the strike-slip regime, as seen in the studied fields, should be guided by geomechanical assessments. Future work should extend the well-based geomechanical modeling into the field scale by integrating a greater number of wells to depict the reservoir geomechanical characteristics field-wide, which will enable the subsurface team to better optimize the drilling and completion strategies.

5. Conclusions

The present study used conventional wireline logs, direct measurements (LOT, formation pressure), and an acoustic image log to ascertain the pore pressure and principal stress magnitudes in the Paleozoic–Mesozoic sedimentary succession of the In-Adaoui and Bourarhat hydrocarbon fields in eastern Algeria. The conclusions of this work are as follows:

- Relative stress magnitudes infer a strike-slip in situ stress state at present with a NW-SE S_{HMax} orientation.
- Pore pressure is dominantly hydrostatic, and there has been no evidence of significant overpressure in the studied interval.
- Being in a strike-slip domain, horizontal wells will be less vulnerable to wellbore failure.
- We infer that the future development well should be drilled parallel to the S_{hmin} azimuth (i.e., NE-SW), so that the hydraulic fractures can propagate along the S_{HMax} direction and create an effective transverse fracture network within the Ordovician reservoirs, which generally exhibit poor permeability.
- Geomechanics-driven drilling optimization and reservoir development strategies are discussed and recommended for the studied fields.

Author Contributions: R.B.: conceptualization, methodology, software, validation, formal analysis, investigation, resources, data curation, writing—original draft preparation, writing—review and editing, visualization. S.S.: conceptualization, methodology, software, validation, formal analysis, investigation, resources, data curation, writing—original draft preparation, writing—review and editing, visualization. A.E.R.: conceptualization, methodology, software, validation, formal analysis, investigation, resources, data curation, writing—original draft preparation, writing—review and editing, visualization, supervision, project administration, funding acquisition. A.A.E.A.: conceptualization, methodology, software, validation, formal analysis, investigation, resources, data curation, writing—original draft preparation, writing—review and editing, visualization. All authors have read and agreed to the published version of the manuscript.

Funding: This research was funded the funding provided by the Priority Research Area Anthropocene under the program "Excellence Initiative—Research University" at the Jagiellonian University in Kraków. The authors are thankful to the deanship of scientific research at Najran University for funding this work under the research groups funding program grant code NU/RG/SERC/12/22.

Data Availability Statement: Not applicable.

Acknowledgments: We are grateful to handling editor, Patricia Persaud (University of Arizona), and the other two reviewers for their constructive review comments that benefited the manuscript. This research was funded by the Priority Research Area Anthropocene under the program "Excellence Initiative—Research University" at the Jagiellonian University in Kraków. R.B. acknowledges the (i) Laboratory of Resources Minérals at Energétiques, University of Boumerdes, and (ii) Directorate General for Scientific Research and Technological Development (DG-RSDT), Ministry of Higher Education and Scientific Research of Algeria, for supporting this research. SONATRACH Company is acknowledged for the well data used here. Pore Pressure and Geomechanics module of GEO Suite of software by Geologix Limited was used for the analyses. The authors are thankful to the deanship of scientific research at Najran University for funding this work under the research groups funding program grant code NU/RG/SERC/12/22.

Conflicts of Interest: The authors declare no conflict of interest.

References

1. Zoback, M.D. *Reservoir Geomechanics*; Stanford University: Stanford, CA, USA, 2007.
2. Baouche, R.; Sen, S.; Boutaleb, K. Present day In-situ stress magnitude and orientation of horizontal stress components in the eastern Illizi basin, Algeria: A geomechanical modeling. *J. Struct. Geol.* **2020**, *132*, 103975. [CrossRef]
3. Baouche, R.; Sen, S.; Sadaoui, M.; Boutaleb, K.; Ganguli, S.S. Characterization of pore pressure, fracture pressure, shear failure and its implications for drilling, wellbore stability and completion design—A case study from the Takouazet field, Illizi Basin, Algeria. *Mar. Pet. Geol.* **2020**, *120*, 104510. [CrossRef]
4. Ganguli, S.S.; Sen, S. Investigation of present-day in-situ stresses and pore pressure in the south Cambay Basin, western India: Implications for drilling, reservoir development and fault reactivation. *Mar. Pet. Geol.* **2020**, *118*, 104422. [CrossRef]
5. Radwan, A.E.; Abdelghany, W.K.; Elkhawaga, M.A. Present-day in-situ stresses in Southern Gulf of Suez, Egypt: Insights for stress rotation in an extensional rift basin. *J. Struct. Geol.* **2021**, *147*, 104334. [CrossRef]
6. Persaud, P.; Pritchard, E.H.; Stock, J.M. Scales of stress heterogeneity near active faults in the Santa Barbara Channel, Southern California. *Geochem. Geophys. Geosyst.* **2020**, *21*, e2019GC008744. [CrossRef]
7. Khan, U.; Zhang, B.; Du, J.; Jiang, Z. 3D structural modeling integrated with seismic attribute and petrophysical evaluation for hydrocarbon prospecting at Dhulian oilfield, Pakistan. *Front. Earth Sci.* **2021**, *15*, 649–675. [CrossRef]
8. Zhang, B.; Tong, Y.; Du, J.; Hussain, S.; Jiang, Z.; Ali, S.; Ali, I.; Khan, M.; Khan, U. Three-dimensional structural modeling (3D SM) and joint geophysical characterization (JGC) of hydrocarbon reservoir. *Minerals* **2022**, *12*, 363. [CrossRef]
9. English, J.M.; Finkbeiner, T.; English, K.L.; Cherif, R.Y. State of Stress in Exhumed Basins and Implications for Fluid Flow: Insights from the Illizi Basin, Algeria. *Geol. Soc. Lond. Spéc. Publ.* **2017**, *458*, 89–112. [CrossRef]
10. Radwan, A.E.; Sen, S. Characterization of in-situ stresses and its implications for production and reservoir stability in the depleted El Morgan hydrocarbon field, Gulf of Suez Rift Basin, Egypt. *J. Struct. Geol.* **2021**, *148*, 104355. [CrossRef]
11. Radwan, A.E. A multi-proxy approach to detect the pore pressure and the origin of overpressure in sedimentary basins: An example from the Gulf of Suez rift basin. *Front. Earth Sci.* **2022**, *10*, 967201. [CrossRef]
12. Baouche, R.; Sen, S.; Boutaleb, K. Distribution of pore pressure and fracture pressure gradients in the Paleozoic sediments of Takouazet field, Illizi basin, Algeria. *J. Afr. Earth Sci.* **2020**, *164*, 103778. [CrossRef]
13. Baouche, R.; Sen, S.; Feriel, H.A.; Radwan, A.E. Estimation of horizontal stresses from wellbore failures in strike-slip tectonic regime: A case study from the Ordovician reservoir of the Tinzaouatine Field, Illizi Basin, Algeria. *Interpretation* **2022**, *10*, SF37–SF44. [CrossRef]
14. Baouche, R.; Ganguli, S.S.; Sen, S.; Radwan, A.E. Assessment of reservoir stress state and its implications for Paleozoic tight oil reservoir development in the Oued Mya Basin, northeastern Algerian Sahara. *Geosystems Geoenvironment* **2023**, *2*, 100112. [CrossRef]
15. Baouche, R.; Sen, S.; Ganguli, S.S.; Boutaleb, K. Petrophysical and geomechanical characterization of the Late Cretaceous limestone reservoirs from the Southeastern Constantine Basin, Algeria. *Interpretation* **2021**, *9*, SH1–SH9. [CrossRef]
16. Baouche, R.; Sen, S.; Radwan, A.E. Geomechanical and Petrophysical Assessment of the Lower Turonian Tight Carbonates, Southeastern Constantine Basin, Algeria: Implications for Unconventional Reservoir Development and Fracture Reactivation Potential. *Energies* **2022**, *15*, 7901. [CrossRef]
17. Baouche, R.; Sen, S.; Ganguli, S.S.; Feriel, H.A. Petrophysical, geomechanical and depositional environment characterization of the Triassic TAGI reservoir from the Hassi Berkine South field, Berkine Basin, Southeastern Algeria. *J. Nat. Gas Sci. Eng.* **2021**, *92*, 104002. [CrossRef]
18. Baouche, R.; Sen, S.; Chaouchi, R.; Ganguli, S.S. Modeling in-situ tectonic stress state and maximum horizontal stress azimuth in the Central Algerian Sahara—A geomechanical study from EL Agreb, EL Gassi and Hassi Messaoud fields. *J. Nat. Gas Sci. Eng.* **2021**, *88*, 103831. [CrossRef]
19. Benayad, S.; Ysbaa, S.; Chaouchi, R.; Haddouche, O.; Kacimi, A.; Kaddour, H. Sedimentological characteristics and reservoir quality prediction in he Upper Ordovician glaciogenic sandstone of the In-Adaoui-Ohanet gas field, Illizi basin, Algeria. *J. Pet. Sci. Eng.* **2019**, *179*, 159–172. [CrossRef]

20. Heidbach, O.; Tingay, M.; Barth, A.; Reinecker, J.; Kurfeß, D.; Müller, B. Global crustal stress pattern based on the World Stress Map database release 2008. *Tectonophysics* **2010**, *482*, 3–15. [CrossRef]
21. Plumb, R.A.; Evans, K.F.; Engelder, T. Geophysical log responses and their correlation with bed to bed stress contrasts in Paleozoic rocks, Appalachian plateau, New York. *J. Geophys. Res.* **1991**, *91*, 14509–14528. [CrossRef]
22. Sen, S.; Corless, J.; Dasgupta, S.; Maxwell, C.; Kumar, M. Issues faced while calculating Overburden gradient and picking shale zone to predict pore pressure. In Proceedings of the First EAGE Workshop on Pore Pressure Prediction, Pau, France, 19–21 March 2017. Paper Mo PP1B 02.
23. Radwan, A.E. Drilling in Complex Pore Pressure Regimes: Analysis of Wellbore Stability Applying the Depth of Failure Approach. *Energies* **2022**, *15*, 7872. [CrossRef]
24. Sen, S.; Ganguli, S.S. Estimation of Pore Pressure and Fracture Gradient in Volve Field, Norwegian North Sea. In Proceedings of the SPE Oil and Gas India Conference and Exhibition, Mumbai, India, 9–11 April 2019. SPE-194578-MS. [CrossRef]
25. Sen, S.; Kundan, A.; Kumar, M. Modeling Pore Pressure, Fracture Pressure and Collapse Pressure Gradients in Offshore Panna, Western India: Implications for Drilling and Wellbore Stability. *Nat. Resour. Res.* **2020**, *29*, 2717–2734. [CrossRef]
26. Sen, S.; Kundan, A.; Kalpande, V.; Kumar, M. The present-day state of tectonic stress in the offshore Kutch-Saurashtra Basin, India. *Mar. Pet. Geol.* **2019**, *102*, 751–758. [CrossRef]
27. Agbasi, O.E.; Sen, S.; Inyang, N.J.; Etuk, S.E. Assessment of pore pressure, wellbore failure and reservoir stability in the Gabo field, Niger Delta, Nigeria—Implications for drilling and reservoir management. *J. Afr. Earth Sci.* **2021**, *173*, 104038. [CrossRef]
28. Radwan, A.E. Modeling pore pressure and fracture pressure using integrated well logging, drilling based interpretations and reservoir data in the Giant El Morgan oil Field, Gulf of Suez, Egypt. *J. Afr. Earth Sci.* **2021**, *178*, 104165. [CrossRef]
29. Matthews, W.R.; Kelly, J. How to predict formation pressure and fracture gradient. *Oil Gas J.* **1967**, *65*, 92–106.
30. Eaton, B.A. Fracture gradient prediction and its application in oilfield operations. *JPT* **1969**, *21*, 25–32. [CrossRef]
31. Barton, C.A.; Zoback, M.D.; Burns, K.L. In-Situ stress orientation and magnitude at the Fenton Geothermal Site, New Mexico, determined from wellbore breakouts. *Geophys. Res. Lett.* **1988**, *15*, 467–470. [CrossRef]
32. Horsrud, P. Estimating Mechanical Properties of Shale from Empirical Correlations. *SPE Drill. Complet.* **2001**, *16*, 68–73. [CrossRef]
33. McNally, G.H.N. Estimation of coal measures rock strength using sonic and neutron logs. *Geoexploration* **1987**, *24*, 381–395. [CrossRef]
34. Zoback, M.D.; Barton, C.A.; Brudy, M.; Castillo, D.A.; Finkbeiner, B.R.; Grollimund, B.R.; Moos, D.B.; Peska, P.; Ward, C.D.; Wiprut, D.J. Determination of stress orientation and magnitude in deep wells. *Int. J. Rock Mech. Min. Sci.* **2003**, *40*, 1049–1076. [CrossRef]
35. Rajabi, M.; Tingay, M.; Heidbach, O. The present-day state of tectonic stress in the Darling Basin, Australia: Implications for exploration and production. *Mar. Pet. Geol.* **2016**, *77*, 776–790. [CrossRef]
36. Heidbach, O.; Rajabi, M.; Reiter, K.; Ziegler, M.; WSM Team. World Stress Map Database Release 2016. *GFZ Data Serv.* **2016**, *V. 1.1*. [CrossRef]
37. Zoback, M.L. First-and second-order patterns of stress in the lithosphere: The World Stress Map Project. *J. Geophys. Res. Solid Earth* **1992**, *97*, 11703–11728. [CrossRef]
38. Soumaya, A.; Ayed, N.B.; Rajabi, M.; Meghraoui, M.; Delvaux, D.; Kadri, A.; Ziegler, M.; Maouche, S.; Braham, A. Active faulting geometry and Stress pattern near complex strike-slip system along the Maghreb region: Constraints on active convergence in the Western Mediterranean. *Tectonics* **2018**, *37*, 3148–3173. [CrossRef]
39. Radwan, A.E.; Sen, S. Stress Path Analysis for Characterization of In Situ Stress State and Effect of Reservoir Depletion on Present-Day Stress Magnitudes: Reservoir Geomechanical Modeling in the Gulf of Suez Rift Basin, Egypt. *Nat. Resour. Res.* **2020**, *30*, 463–478. [CrossRef]
40. DeMets, C.; Gordon, R.G.; Argus, D.F.; Stein, S. Effect of recent revisions to the geomagnetic reversal time scale on estimates of current plate motions. *Geophys. Res. Lett.* **1994**, *21*, 2191–2194. [CrossRef]